

Luminescent properties of crystalline lithium triborate LiB_3O_5

I. N. Ogorodnikov and A. V. Kruzhakov

Ural State Technical University, 620002 Ekaterinburg, Russia

E. A. Radzhabov

Institute of Geochemistry, Siberian Branch of the Russian Academy of Sciences, 664033 Irkutsk, Russia

L. I. Isaenko

Single-Crystal Institute, Siberian Branch of the Russian Academy of Sciences, 630058 Novosibirsk, Russia
 (Submitted June 4, 1998)

Fiz. Tverd. Tela (St. Petersburg) **41**, 223–228 (February 1999)

A study of the luminescence characteristics of crystalline lithium triborate LiB_3O_5 (LBO) is reported. Investigation of the excitation and photoluminescence spectra of nominally pure, oriented LBO crystals within broad spectral (1.2–10.5 eV) and temperature (8–500 K) regions, complemented by optical spectroscopy at the long-wavelength fundamental-absorption edge, has revealed that the broad-band LBO luminescence in the 3.5–4.5-eV region is efficiently excited by photons having energies above 7.5 eV in recombination processes and under corpuscular or x-ray irradiation. The totality of the experimental data obtained permitted a conclusion that the LBO luminescence has an intrinsic nature and that it originates from radiative decay of relaxed electronic excitations. © 1999 American Institute of Physics.
 [S1063-7834(99)00802-3]

Many wide-gap insulators are characterized by strong electron-phonon coupling, which accounts for a substantial part of lattice relaxation and provides favorable conditions for self-trapping of electronic excitations (EE). One discriminates between two main channels of self-trapped exciton (STE) formation, namely, via a recombination process or by direct excitation of the resonant exciton with its subsequent relaxation. In cubic alkali-halide crystals, both mechanisms can initiate formation of STEs of the same type.¹ In lower-symmetry crystals [e.g., BeO ,² Al_2O_3 , YAlO_3 , $\text{Y}_3\text{Al}_5\text{O}_{12}$ (Ref. 3)] STEs of two types differing in properties are observed to coexist. The fundamental reasons for this lie in different patterns of relaxation that the lattice undergoes in the cases of charged (recombination) and electrically neutral EE in low-symmetry crystals, where charge self-trapping occurring in the first stage of STE formation in the recombination process perturbs substantially the Coulomb field of the crystal, as contrasted to the relaxation of a resonant exciton. The complex crystal structure of many low-symmetry insulators suggests existence of a large number of lattice relaxation paths, which in some cases results in stabilization of various final states⁴ and makes it difficult to establish the nature of the relaxation processes in these compounds.

There is presently a considerable interest in the investigation of the dynamics of electronic excitations in nonlinear crystalline borates of some alkali metals [$\beta\text{-BaB}_2\text{O}_4$ (BBO), LiB_3O_5 (LBO), CsB_3O_5 (CBO), and $\text{Li}_2\text{B}_4\text{O}_7$], which enjoy broad application in present-day nonlinear and integrated optics as converting and waveguide optical media. Some crystals of this group [$\beta\text{-BaB}_2\text{O}_4$ (Ref. 5), $\text{Li}_2\text{B}_4\text{O}_7$ (Ref. 6)] exhibit a fairly strong short-wavelength intrinsic lumines-

sence, which is assigned to radiative annihilation of self-trapped EEs or radiative decay of relaxed EEs at lattice defects. The luminescence of these crystals has a number of common features, and it is efficiently excited both by photons at the long-wavelength fundamental-absorption edge (LWAE) and in recombination processes. LBO crystals have been overlooked in this respect until recently, and filling in this gap would be of considerable interest from the standpoint of establishing common features in the dynamics of EEs and of the luminescence in crystals of this group and their relation with those observed in more thoroughly studied wide-gap insulators.

Lithium triborate LiB_3O_5 has a complex orthorhombic cell containing four formula units, with space group $Pn2_1a$ and lattice parameters $a = 8.46 \text{ \AA}$, $b = 5.13 \text{ \AA}$, and $c = 7.38 \text{ \AA}$. Two of the three inequivalent boron atoms have a plane threefold-coordinated bond structure similar to that of B_2O_3 . The third boron atom has a tetrahedral, fourfold-coordinated bond structure. There are five inequivalent oxygens. The crystal structure represents a boron-oxygen framework containing lithium atoms in open voids.⁷ The LBO transmission band extends from 159 to 3500 nm.⁸

We detected earlier⁹ UV luminescence of LBO crystals, which can be excited by both x-ray photons and an electron beam with an energy $E_e = 0.15 \text{ MeV}$. Subsequent investigation revealed some features, in particular, a complex luminescence-band profile, and participation of the main point defects in its excitation by recombination, which is to be contrasted with the absence of a clearly pronounced relation with the existence in the LBO lattice of any activator.^{10,11} This gave grounds for the conjecture of the

LBO luminescence being of intrinsic origin.¹² Proving this would require, however, a comprehensive study of the excitation and photoluminescence of LBO, as well as of the LWAE.

This work was aimed at a study of the excitation and photoluminescence spectra of nominally pure LiB_3O_5 crystals within broad spectral and temperature regions, complemented by optical spectroscopy of LBO at the LWAE.

1. EXPERIMENTAL TECHNIQUES

LiB_3O_5 crystals were grown by crystallization from a $\text{Li}_2\text{O}-\text{B}_2\text{O}_3-\text{MoO}_3$ melt with the seed in the upper position. The starting materials of OSCh grade, up to 400 cm^3 in volume, were placed in a platinum crucible, so that the content of LiB_3O_5 in the system was 30–35 wt%. After homogenization and a pause at $850-900^\circ\text{C}$, the melt was cooled down to the saturation temperature, and the seed crystal was brought in contact with the surface. The single crystals were grown with [010] orientation at a cooling rate of 0.1–0.2 K/h. A typical LBO crystal grown for 15–20 days varied from 70 to 120 g in weight.

We used a set of 10 nominally pure LBO crystals of optical quality in the form of polished plane-parallel plates measuring $10 \times 10 \times 1.5 \text{ mm}$, with the plane perpendicular to the X or Z crystallographic axes. For brevity, they are denoted by $\text{LBO} \perp \mathbf{X}$ and $\text{LBO} \perp \mathbf{Z}$, respectively.

The luminescence measurements were performed on an experimental setup including a VMR-2 vacuum monochromator with a 600-l/mm spherical grating, a high collecting-power MDR-2 monochromator with a 1200-l/mm grating, FÉU-106 and FÉU-142 PM tubes operating in the photon counting mode, a VMF-25 hydrogen lamp as a source of VUV light, an evacuated optical chamber with a LiF window provided with a low-inertia cryostat having interchangeable units for operation within a broad temperature range from 8 to 600 K, and an oil-free pumping system. The luminescence emitted in studies of excitation spectra was passed through a UFS-2 filter. The x-ray luminescence was excited with a BSV-2 tube ($U_a = 30 \text{ kV}$, $I_a = 10 \text{ mA}$, Cu anticathode). The output formatted in the CAMAC standard was interfaced to a computer providing control of the various assemblies and data acquisition and processing.

2. RESULTS OF EXPERIMENT

Measurements of LBO optical-absorption (OA) spectra showed the monotonic exponential growth of optical absorption in unirradiated crystals to start above 7.5 eV (Fig. 1), with no OA bands observed within the LBO transmission region. It was found that the real position of LWAE depends both on temperature and on the crystallographic orientation of the sample. For instance, the LWAE position in all $\text{LBO} \perp \mathbf{Z}$ crystals was shifted by about 150 meV toward shorter wavelengths compared to that for $\text{LBO} \perp \mathbf{X}$ crystals (Fig. 1). A change in crystal temperature from room temperature to 80 K shifts the LWAE toward shorter wavelengths in all cases by about 100 meV (Fig. 1). Irradiation of LBO by a 150-keV electron beam creates lattice defects of several types. Low-temperature defects responsible for opti-

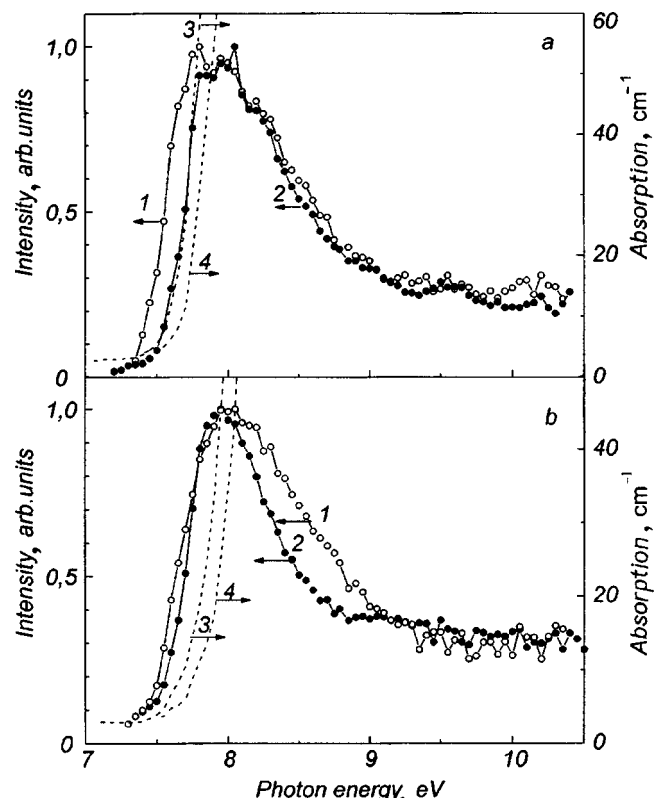


FIG. 1. Excitation spectra of (1,2) luminescence and (3,4) optical absorption of (a) $\text{LBO} \perp \mathbf{X}$ sample and (b) $\text{LBO} \perp \mathbf{Z}$ sample obtained at (1,3) 290 K and (2,4) 80 K.

cal absorption in the transmission region of the crystal were studied in Ref. 13. Our study reports on detection of high-temperature LBO lattice defects, which persist above 650 K and manifest themselves in OA spectra close to the LWAE (Fig. 2). The nature of the high-temperature defects remains unclear. For our present work it is essential that no photoluminescence is observed under optical excitation within the OA band of either low- or high-temperature LBO defects.

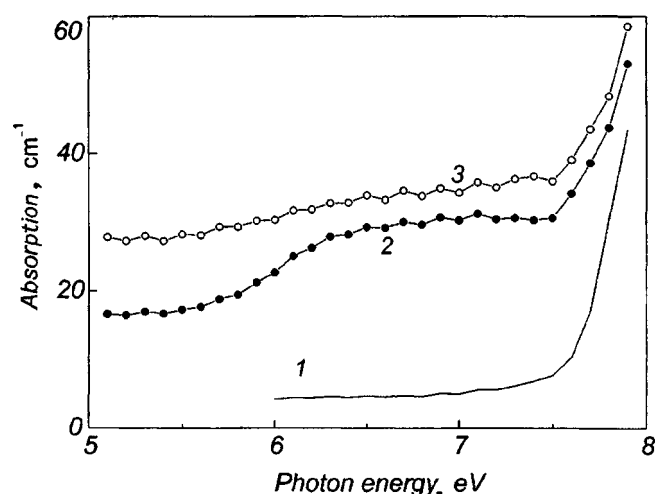


FIG. 2. Optical absorption spectra of LBO obtained at 300 K: 1 — before irradiation, 2 — after irradiation by a 150-keV electron beam, 3 — after annealing the irradiated sample in air at 650 K.

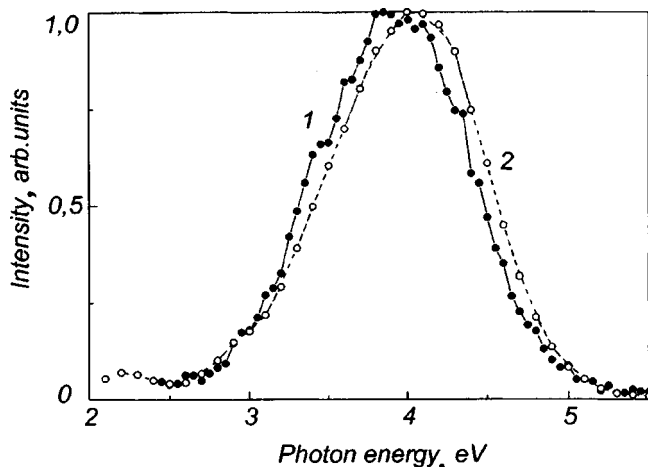


FIG. 3. Luminescence spectra of LBO obtained at 290 K under excitation with (1) photons with energy $E_{ex} = 7.7$ eV and (2) x-ray photons.

By contrast, excitation of unirradiated LBO by photons with energies above 7.5 eV gives rise to the appearance of broad-band photoluminescence (PL) within the 2.5–4.5-eV region (Fig. 3). The excitation spectrum of this luminescence is a strong band peaking near 7.9–8.0 eV. The long-wavelength edge of the excitation spectrum rises steeply in the 7.5–8.0-eV region to its maximum, followed by a smooth falloff to a constant level of 20–25% of the maximum value, to remain afterwards practically unchanged within the 9.5–10.5-eV spectral interval (Fig. 1). As seen from Fig. 1, the profile of the excitation band depends both on temperature and on the crystallographic orientation of the sample. For instance, at 80 K the excitation-band profiles measured for $LBO \perp X$ and $LBO \perp Z$ crystals coincide fairly well to form a band peaking at 8.0 eV with a FWHM of about 0.8 eV, whereas at 290 K they are noticeably broader. Also, in $LBO \perp Z$ crystals the broadening by about 200 meV occurs at the short-wavelength falloff of the excitation band with its long-wavelength decay remaining practically unchanged, while the situation in $LBO \perp X$ crystals is different, namely, a similar broadening of the excitation band takes place only at the long-wavelength decline (Fig. 1).

Most of the PL spectrum is confined to a Gaussian-shaped band with a FWHM of 1.2 eV peaking at 4.0 eV (Fig. 3). The LBO luminescence band has the same shape when excited at different points within the 7.7–10.5-eV spectral region. Figure 3 shows also an x-ray-excited LBO luminescence spectrum, which is seen to be close in shape to the PL spectrum.

It should be pointed out that the luminescence spectrum contains features in the form of weak shoulders superimposed on the main band profile (Fig. 3). These features vary in intensity and position from one sample to another, depend on the temperature regime used and other experimental conditions. For example, cooling to 77 K gives rise to a noticeable luminescence in the 2.5–4.5-eV region, which appears without any external irradiation and coincides in its main characteristics with the PL spectrum. Following a few hours' maintenance in vacuum in the dark, the spontaneous luminescence in LBO dies out completely. Note that heating an

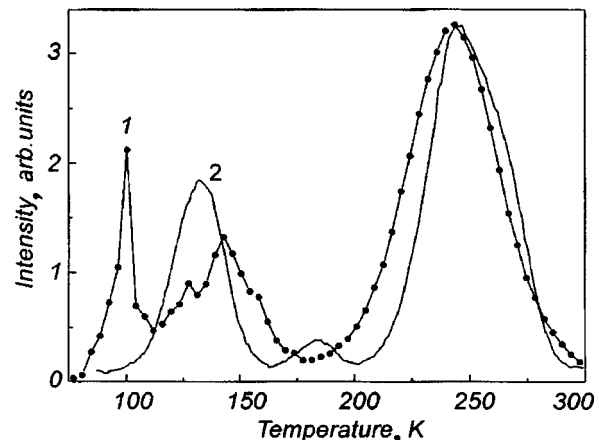


FIG. 4. (1) Luminescence of an unirradiated sample heated in vacuum at a rate of 5 K/s and (2) thermostimulated luminescence of LBO irradiated by x-rays at 77 K.

unirradiated sample within the 80–200 K interval at a rate faster than 5 K/s likewise initiates spontaneous emission, whose intensity depends on the heating rate and can become higher than that of the PL by one to two orders of magnitude. No such luminescence was observed to occur above 200 K. Interestingly, in unirradiated samples this results in generation of carriers, their localization at higher-temperature trapping centers, and subsequent thermally stimulated luminescence (TSL) near the well-known TSL peak at 240 K (Fig. 4). Such thermally induced light flashes are characteristic of many pyroelectric crystals, in particular, of lithium tetraborate.⁶ Investigation of the nature of this luminescence would require an independent study involving an analysis of lattice dynamics. We shall focus our attention here on the main part of the PL spectrum, which is not affected by the above nonisothermal phenomena.

To remove these effects in measurements of the temperature dependence of the PL, we used heating and cooling rates below 0.05 K/s. PL spectra measured at 8 and 80 K coincide in shape with that obtained at room temperature (Fig. 3). The PL intensity measured at 77 K exceeds typically that taken at room temperature two times. Figure 5 displays the temperature dependence of the PL intensity in the 8–400 K range, which follows Mott's law with $E_a = 290$ meV and $\omega = 2.4 \times 10^5$ s⁻¹. The luminescence is thermally quenched above 240 K. With allowance made for the temperature-induced shift of the PL excitation band, the temperature dependence of PL was found to be the same for different energies of exciting photons.

The temperature dependence of the x-ray induced luminescence follows a somewhat different pattern. It does not typically exhibit thermally induced light emission. Above 240 K, it undergoes temperature quenching coinciding with that for the PL, whereas when cooled from 240 to 80 K, the PL intensity drops 20–25 times (Fig. 5). The reason for this lies in carrier localization at the electronic, B^{2+} , and hole, O^- , trapping centers having characteristic carrier delocalization temperatures of 130 and 240 K, respectively.

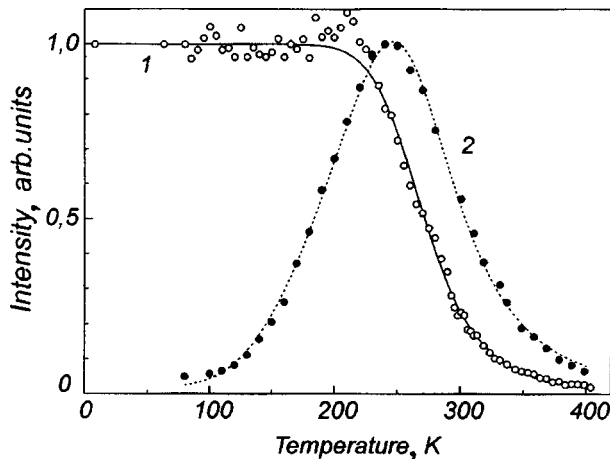


FIG. 5. Temperature dependences of (1) photoluminescence of unirradiated LBO samples at $E_{ex} = 7.7$ eV and (2) x-ray luminescence. Points - experimental data, lines - assumed theoretical relations.

3. DISCUSSION OF RESULTS

The experimental data obtained reveal primarily a large, as high as 4 eV, Stokes shift of LBO photoluminescence and a correlation between the sharp increase of the crystal optical density for photon energies in excess of 7.5 eV and the profile of the long-wavelength edge of the PL excitation spectrum (Fig. 1). The increase in OA above the 7.5-eV photon energy should be assigned to fundamental absorption in LBO. Indeed, despite the fact that the exact value of E_g for LBO is still a subject of controversy, both experimental and theoretical estimates of E_g from the absorption edge yield values from 7.75 to 7.80 eV.^{8,14,15} At the same time LBO band-structure calculations suggest $E_g = 7.37$ eV in the Γ - Γ direction.¹⁶ This is not contradicted by LBO reflectance-spectrum studies done for the 6–12-eV region and by the corresponding calculations^{17,18}, by which the energy of the $4a_2$ orbital assigned to the lower conduction band is 7.3 eV.

In this connection, experimental data (Fig. 1) permit a conclusion that the longest-wavelength fundamental-absorption peak of LBO crystals lies above 7.7 or 7.9 eV, depending on the sample crystallographic orientation. This is in full agreement with the value of 7.78 eV obtained earlier⁸ for nonoriented LBO samples and accepted as an estimate of E_g . It should be pointed out that optical absorption of LBO grows steeply in the immediate vicinity of the gap edge, which differs essentially from the situation observed in other borates (BBO, CBO), where interband transitions at the extremal points are forbidden by symmetry considerations and fundamental optical absorption becomes observable at energies slightly in excess of E_g .⁸ A more careful analysis of the fundamental-absorption edge at different temperatures (Fig. 1) indicates that it can be fitted well by a Lorentzian. The optical density at the maximum of this absorption band can be approximately estimated as 10^4 cm^{-1} , which is a fairly large value. Such properties can imply the presence at the LBO absorption edge of exciton-like electronic excitations, which probably overlap with interband transitions.

At the same time, in contrast to alkali-halide crystals and some binary oxides [for instance, BeO (Ref. 19)], the investi-

gation of the LBO near the liquid-helium temperature performed in this work did not reveal any luminescence near the absorption edge that could be assigned to these states. Such pattern is typical of some simple oxides (for example, MgO and Al_2O_3) and can be realized apparently in BBO (Ref. 5) and $\text{Li}_2\text{B}_4\text{O}_7$ (Ref. 20). This interpretation is supported by the shape of the LBO luminescence excitation spectrum in the fundamental absorption region of the crystal, which is typical of crystals producing excitonic-like luminescence, as well as by its characteristic temperature dependence, the large emission band width, and a considerable Stokes shift. In this connection, LBO luminescence can be associated with radiative annihilation of relaxed exciton-like electronic excitations, as is the case with BBO (Ref. 5) and $\text{Li}_2\text{B}_4\text{O}_7$ (Ref. 20), or with the emission of relaxed excitons localized at small-scale structural distortions²¹. Additional arguments could come from studies of the electronic structure of LBO and simulation of the optical characteristics of borates.

The numerous LBO band-structure^{8,14,16,22} and cluster¹⁵ calculations, as well as XPS data obtained for this crystal^{18,23} indicate unambiguously that the valence-band structure of LBO derives primarily from anionic states. Boron ions contribute comparatively little to the valence- and conduction-band states, whereas lithium-ion states do not participate in the electronic structure of the LBO valence band at all. In this connection, the electronic states of LBO are dominated by localized boron-oxygen bonds. The calculations suggest also that the LBO bands have a small dispersion in K space and that the valence band, in particular, has minigaps throughout the wave-vector variation range. As a result, the carrier effective mass is fairly large and is estimated as 0.73, 0.89, and 0.69 m_e for the conduction-band directions Γ - X , Γ - S , and Γ - Z , respectively.¹⁶

An analysis of possible electronic transitions from the upper valence to the lower conduction band showed them to be dominated by the electronic structure of the boron-oxygen groups, and this situation is typical of the LBO, CBO, and BBO crystals. A recent LAPW band-structure calculation²² made for all crystals in this group showed their valence-band top to derive primarily from the oxygen orbitals, with boron ions contributing practically nothing. Note that the lowest-energy electronic transition in LBO occurs to the states evolving from the trigonally hybridized orbitals of the boron and oxygen ions forming the bottom of the conduction band. By contrast, in the other borates (CBO and BBO) the conduction-band bottom derives from the cation states, and transitions from valence-band states due to oxygen ions to purely cationic states at the conduction band-bottom have a comparatively low probability. Stronger transitions are seen at about 1 eV above the absorption edge, where mixed boron-oxygen orbitals of the CBO and BBO crystals become involved in formation of the final state of the interband transition.

Taking into account all the above-mentioned considerations, namely, that the excitation spectrum lies within the fundamental absorption region and is characterized by a higher efficiency at the long-wavelength edge, thermal stimulation of recombination processes, and the temperature dependences of x-ray and photoluminescence, one may con-

clude that the LBO luminescence is an intrinsic process originating from radiative annihilation of relaxed exciton-like electronic excitations, which can form either directly or in recombination involving the main lattice defects.

Thus the present studies of the photoluminescence and photoexcitation of LBO crystals give us grounds to associate the broad-band photoluminescence peaking at 3.75–3.8 eV with the intrinsic luminescence of LBO, which originates from radiative annihilation of relaxed exciton-like electronic excitations. Viewed from the standpoint of possible applications, this luminescence can be used in nondestructive testing of optical components made of LBO and subject to heavy laser-radiation loads.

O. I. N. and K. A. V. owe their thanks to Ch. B. Lushchik for performing some measurements at helium temperatures and for critical comments on some aspects of the work.

Support of the INCO-COPERNICUS program (Grant IC15-CT96-0721) is gratefully acknowledged.

- ¹Ch. B. Lushchik and A. Ch. Lushchik, *Decay of Electronic Excitations with Formation of Defects in Solids* [In Russian] (Nauka, Moscow, 1989), 264 pp.
- ²I. N. Ogorodnikov, V. Yu. Ivanov, and A. V. Kruzhakov, *Fiz. Tverd. Tela* (St. Petersburg) **36**, 3287 (1994) [Phys. Solid State **36**, 1748 (1994)].
- ³A. I. Kuznetsov, V. N. Abramov, V. V. Myurk, and B. R. Namozov, *Fiz. Tverd. Tela* (Leningrad) **33**, 2000 (1991) [Sov. Phys. Solid State **33**, 1126 (1991)].
- ⁴V. Mürk and N. Yaroshevich, *J. Phys.: Condens. Matter* **7**, 5857 (1995).
- ⁵V. Kisand, R. Kink, M. Kink, J. Maksimov, M. Kirm, and I. Martinson, *Physica Scripta* **54**, 542 (1996).
- ⁶O. T. Antonyak, Ya. V. Burak, I. T. Lyseiko, N. S. Pidzrailo, and Z. A. Khapko, *Opt. Spektrosk.* **61**, 550 (1986) [Opt. Spectrosc. **61**, 345 (1986)].
- ⁷S. F. Radaev, N. I. Sorokin, and V. I. Simonov, *Fiz. Tverd. Tela* (Leningrad) **33**, 3597 (1991) [Sov. Phys. Solid State **33**, 2024 (1991)].

- ⁸R. H. French, J. W. Ling, F. S. Ohuchi, and C. T. Chen, *Phys. Rev. B* **44**, 8496 (1991).
- ⁹I. N. Ogorodnikov, V. Yu. Ivanov, A. Yu. Kuznetsov, A. V. Kruzhakov, V. A. Maslov, and L. A. Ol'khovaya, *Pis'ma Zh. Tekh. Fiz.* **19**, No. 2, 14 (1993) [Tech. Phys. Lett. **19**, 42 (1993)].
- ¹⁰I. N. Ogorodnikov, A. Yu. Kuznetsov, A. V. Kruzhakov, and V. A. Maslov, *Radiat. Meas.* **24**, 423 (1995).
- ¹¹I. N. Ogorodnikov, A. V. Porotnikov, V. A. Pustovarov, and A. V. Kruzhakov, *J. Lumin.* **72-74**, 703 (1997).
- ¹²I. N. Ogorodnikov, V. A. Pustovarov, A. V. Porotnikov, and A. V. Kruzhakov, *Nucl. Instrum. Methods Phys. Res. A* **404**, 339 (1995).
- ¹³I. N. Ogorodnikov, A. V. Porotnikov, S. V. Kudyakov, A. V. Kruzhakov, and V. Yu. Yakovlev, *Fiz. Tverd. Tela* (St. Petersburg) **39**, 1535 (1997) [Phys. Solid State **39**, 1366 (1997)].
- ¹⁴W. Y. Hsu and R. V. Kasowski, *J. Appl. Phys.* **73**, 4101 (1993).
- ¹⁵A. B. Sobolev, A. Yu. Kuznetsov, I. N. Ogorodnikov, and A. V. Kruzhakov, *Fiz. Tverd. Tela* (St. Petersburg) **36**, 1517 (1994) [Phys. Solid State **36**, 829 (1994)].
- ¹⁶Y.-N. Xu and W. Y. Ching, *Phys. Rev. B* **41**, 5471 (1990).
- ¹⁷T.-J. Chen, R. N. Zitter, R. Tao, W. R. Hunter, and J. C. Rife, *Phys. Rev. B* **52**, 13703 (1995).
- ¹⁸T.-J. Chen, R. Tao, J. C. Rife, and W. R. Hunter, *J. Opt. Soc. Am. B* **15**, 47 (1998).
- ¹⁹I. N. Ogorodnikov and A. V. Kruzhakov, *J. Lumin.* **72-74**, 701 (1997).
- ²⁰V. N. Kolobanov, J. Becker, S. Downs, B. I. Zadneprovskii, I. A. Kamenskikh, A. Karl, V. V. Mikhaïlin, V. A. Nefedov, M. Runne, D. Tikhon, I. N. Shpin'kov, and H. Zimmerer, in *Abstracts, 1st All-Russia Symposium on SSD* (Ekaterinburg, 1997), p. 94.
- ²¹D. Visser, G. C. Verschoor, and D. J. W. Jido, *Acta Crystallogr., Sect. B: Struct. Crystallogr. Cryst. Chem.* **36**, 28 (1980).
- ²²J. Li, C.-g. Duan, Z.-q. Gu, and D.-s. Wang, *Phys. Rev. B* **57**, 6925 (1998).
- ²³A. Yu. Kuznetsov, M. V. Kuznetsov, I. N. Ogorodnikov, A. V. Kruzhakov, and V. A. Maslov, *Fiz. Tverd. Tela* (St. Petersburg) **36**, 845 (1994) [Phys. Solid State **36**, 465 (1994)].

Translated by G. Skrebtsov